An Optimized Swinging Door Algorithm for Wind Power Ramp Event Detection

Preprint

Mingjian Cui[1] Jie Zhang[2], Anthony R. Florita[2], Bri-Mathias Hodge[2], Deping Ke[1], and Yuanzhang Sun[1]

[1] Wuhan University
[2] National Renewable Energy Laboratory

Presented at the IEEE Power and Energy Society General Meeting
Denver, Colorado
July 26–30, 2015

NREL is a national laboratory of the U.S. Department of Energy
Office of Energy Efficiency & Renewable Energy
Operated by the Alliance for Sustainable Energy, LLC

This report is available at no cost from the National Renewable Energy Laboratory (NREL) at www.nrel.gov/publications.

Conference Paper
NREL/CP-5D00-63877
August 2015

Contract No. DE-AC36-08GO28308

This report is available at no cost from the National Renewable Energy Laboratory (NREL) at www.nrel.gov/publications.

Available electronically at SciTech Connect http:/www.osti.gov/scitech

Available for a processing fee to U.S. Department of Energy and its contractors, in paper, from:

U.S. Department of Energy
Office of Scientific and Technical Information
P.O. Box 62
Oak Ridge, TN 37831-0062
OSTI http://www.osti.gov
Phone: 865.576.8401
Fax: 865.576.5728
Email: reports@osti.gov

Available for sale to the public, in paper, from:

U.S. Department of Commerce
National Technical Information Service
5301 Shawnee Road
Alexandria, VA 22312
NTIS http://www.ntis.gov
Phone: 800.553.6847 or 703.605.6000
Fax: 703.605.6900
Email: orders@ntis.gov

Cover Photos by Dennis Schroeder: (left to right) NREL 26173, NREL 18302, NREL 19758, NREL 29642, NREL 19795.

NREL prints on paper that contains recycled content.

An Optimized Swinging Door Algorithm for Wind Power Ramp Event Detection

Mingjian Cui, *Student Member*, *IEEE*, Jie Zhang, *Member, IEEE*, Anthony R. Florita, *Member, IEEE*,
Bri-Mathias Hodge, *Member*, *IEEE*, Deping Ke, and Yuanzhang Sun, *Senior Member*, *IEEE*

***Abstract*—Significant wind power ramp events (WPREs) are those that influence the integration of wind power, and they are a concern to the continued reliable operation of the power grid. As wind power penetration has increased in recent years, so has the importance of wind power ramps. In this paper, an optimized swinging door algorithm (SDA) is developed to improve ramp detection performance. Wind power time series data are segmented by the original SDA, and then all significant ramps are detected and merged through a dynamic programming algorithm. An application of the optimized SDA is provided to ascertain the optimal parameter of the original SDA. Measured wind power data from the Electric Reliability Council of Texas (ERCOT) are used to evaluate the proposed optimized SDA. Results show that the proposed optimized SDA method provided better performance than the L1-Ramp Detect with Sliding Window (L1-SW) method but with significantly less (almost 1,400 seconds less) computational requirements, and it was also used as a baseline to determine the optimal value of the tunable parameter in the original SDA for ramp detection.**

***Index Terms*—Dynamic programming, swinging door algorithm, sliding window, wind power ramp events, ERCOT**

NOMENCLATURE

J	objective function
$S(i, j)$	score function of the time interval (i, j)
$R(i, j)$	rule sets of the time interval (i, j)
$E_{(\cdot)}$	time interval of WPRE
p_t	wind power generation at time t
t_{ws}	start time point of sliding window
t_{we}	end time point of sliding window
$s_{(\cdot)}$	start time of WPRE
$e_{(\cdot)}$	end time of WPRE
L	number of optimized significant ramp events
$L_{(\cdot)}$	length of sliding window
M	number of sliding windows
ε	only tunable parameter in SDA
ε_{opt}	optimal parameter in SDA
λ	penalty parameter in L1-SW
γ	second derivative threshold in L1-SW

I. INTRODUCTION

The variability and uncertainty associated with wind power presents new challenges for the economic and reliable operation of the power grid [1], [2]. Large fluctuations in wind power in a short period, that are of a significance deemed relative to the plant's capacity or local renewable penetration will form wind power ramp events [3-5]. Significant ramp events are particularly important in the management and dispatch of wind power as part of a portfolio of renewable and non-renewable generation. Traditional generators must regulate their output to compensate for substantial changes in wind power. This can be done by using grid ancillary services or restricting wind turbine output, a process known as curtailment; however, these measures have economic consequences to power grid operation. Ramp event forecasting has the potential to alleviate some economic inefficiencies by helping power system operators plan more economic ancillary decisions.

Reference [6] defined a family of scoring functions for ramp events and used a dynamic programming recursion technique to detect them. Reference [7] used a swinging door algorithm (SDA) [8] to derive three parameters for each wind power interval: ramping capability, ramping rate, and ramping duration. Reference [9] applied an SDA to identify variable generation ramping events from historical wind and solar power data. Reference [10] adopted an SDA to extract ramp events from actual and forecasted wind power and to evaluate the performance of improved short-term wind power forecasts.

The organization of this paper is as follows. The formulation of the optimized SDA is presented in Section II. The experimental results of a case study are discussed in Section III. In Section IV, the proposed optimized SDA is used as a baseline for tuning the parameters in the original SDA. Section V concludes the paper.

II. OPTIMIZED SWINGING DOOR ALGORITHM

A. *Original Swinging Door Algorithm*

To detect any significant ramps, the original SDA [8], [11] has been adapted to extract ramp periods in a time series of wind power data. This algorithm is based on the concept of a "swinging door" with a "turning point" (i.e., at time 0 with magnitude 5, as shown in Fig. 1(a)) whenever the next point in the time series causes any intermediate point to fall outside the area partitioned by the up and down segment bounds. The segment bounds are defined by the door width $\pm\varepsilon$, which is the only tunable parameter in the SDA. More detailed descriptions of the original SDA can be found in [7], [9]-[10]. For example, points A, B, and C are all inside the segment bounds determined by Point D with $\pm\varepsilon$. After segmenting the wind power signal by the original SDA, the wind power ramp events (WPREs) are extracted according to the user-specified definition of a significant ramp.

An example of a ramp detection by the SDA is shown in Fig. 1(b). There is one significant up-ramp (20^{th} hour–28^{th} hour) and one significant down-ramp (28^{th} hour–40^{th} hour) rather than two up-ramps and three down-ramps, as would be detected using a suboptimal door, ε, width value. Similar observations can also be seen from the 50^{th} hour to 60^{th} hour. This phenomenon motivates the development of an optimized SDA, which can combine adjacent up-ramps (or down-ramps) to improve the behavior of the original SDA.

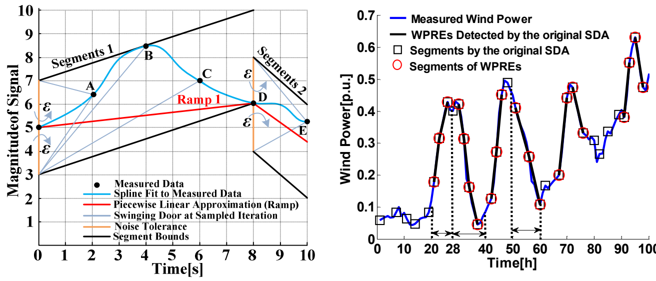

(a) (b)

Fig. 1. (a) The swinging door algorithm for the detection of ramps in wind power from the time series [9]; (b) Detected WPREs by the original SDA and corresponding segments with ε=0.9%.

B. Optimized Swinging Door Algorithm Based on a Dynamic Programming Approach

The objective of the optimization approach is to minimize the number of individual ramps while still approximating the wind power signal as a ramp. Therefore, adjacent segments with the same slope (e.g., up-ramps) can be merged into one segment. To this end, an optimization process is performed to the original segments (from the original SDA) using a dynamic programming algorithm. Dynamic programming is a method for solving a complex problem by breaking it down into a collection of simpler subproblems. Every subinterval (subproblem) that satisfies ramp rules is rewarded a positive score that forms an increasing function S of the length of one subinterval segmented by the original SDA. The optimization problem seeks to maximize the length score function, which corresponds to a set of subintervals (complex problem). More detailed descriptions and demonstrations of dynamic programming are shown in [6].

Given a wind power interval (i, j) of all discrete time points and an objective function J of the dynamic programming model, a WPRE is detected by maximizing the objective function:

$$J(i, j) = \max_{i<k\leq j}[S(i, k) + J(k, j)],\ i < j \tag{1}$$

where $J(i, j)$ is the maximum score in interval (i, j), which can be computed as the maximum over $(i - j)$ subproblems. The term of $S(i, k)$ is a positive score value corresponding to the interval (i, k), which conforms to a super-additivity property:

$$S(i, j) > S(i, k) + S(k + 1, j),\ \forall i < k < j \tag{2}$$

An entire family of score functions satisfies (2), and the score function presented in [6] is adopted in this paper, expressed as:

$$S(i, j) = (j - i)^2 \times R(i, j) \tag{3}$$

where $R(i, j)$ is the definition of a ramp in the interval (i, j). This definition $R(i, j)$ in (3) has been extensively used in the literature [12]-[13]. Significant wind power ramps can be defined based on the power change magnitude, direction, and duration. Three definitions proposed in [10] are investigated in this paper. If $R(i, j)$ conforms to the threshold of ramp definitions, $R(i, j)$ is assigned to be 1; otherwise, $R(i, j)$ is assigned to be 0. The overall process of the optimized SDA is described in Fig. 2.

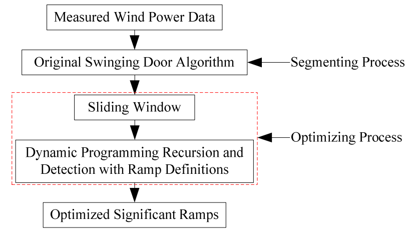

Fig. 2. The overall process of the optimized SDA.

In Fig. 2, there are M sliding windows with the start point (t_{ws}, p_{ws}) and the end point (t_{we}, p_{we}). A set of significant ramps E_i will be detected in each window where $E_i = (s_i, e_i)$ with the start (s_i) and end (e_i). The number of significant ramps in each window may be different (e.g., the first window with L_1 and the last window with L_M).

In brief, all the segments (represented by the square points in Fig. 1(b)) are first extracted by the original SDA with a predefined parameter ε. Then all extracted segments are input into the optimization procedure (the red block in Fig. 2). The extracted segments are merged to yield the set of optimized significant ramp events $(s_1, e_1), ..., (s_\mathrm{L}, e_\mathrm{L})$. Numerical results of the optimized SDA are shown in Section III.

III. Experimental Results

A. Data Description

The optimized SDA detection scheme was applied to measured wind power data from the Wind Forecasting Improvement Project (WFIP) Southern Study [14], covering most of the Electric Reliability Council of Texas (ERCOT) service area. The WFIP southern study region included 8,296 MW of wind capacity spread among 84 wind power plants. A set of data with different time resolutions (1 h and 15 min) are for a nearly 12-month period spanning from October 2011 to mid-September 2012. Because the parameter ε can automatically characterize the threshold sensitivity to noise, data preprocessing of the noise was not necessary.

B. Comparison to an Optimal Wind Power Ramp Event Detection Method

A detection method for WPREs was developed recently by [6], [15], referred as “L1-Ramp Detect with Sliding Window” (L1-SW), to characterize the ramp start times, durations, rates, and other key features needed in the operation of a power system. Unlike the optimized SDA, using the original SDA for segmentation, the segmented process of the L1-SW method uses L1 trend fitting with a penalty parameter λ and the second derivative with a threshold γ. The L1-SW method is capable of smoothing the noise in wind power and subsequently segmenting the wind power into piecewise data. In this subsection, a significant ramp is defined as the change in wind power that is greater than 10% of the installed wind capacity [10]. Note that this threshold (10%) is set smaller to extract sufficient ramps for the comparison of the L1-SW to the optimized SDA (shown in Figs. 3 and 4).

Figs. 3(a) and 3(b) compare the segments approximated by the L1-SW to the optimized SDA methods with different parameter values. The parameter ε in the optimized SDA is set to be 0.009 in the both Figs. 3(a) and 3(b); the parameter λ is set to be 0.5 in L1-SW and 0 in Figs. 3(a) and 3(b), respectively. Figs. 3(c) and 3(d) compare the significant ramps extracted by the two methods. Fig. 3(c) corresponds the segments shown in Fig 3(a); Fig 3(d) corresponds the segments shown in Fig 3(b).

Fig. 3(a) indicates that segments of the optimized SDA are more accurate than that of L1-SW with a larger λ. For example, as shown in the intervals of the 65th hour–120th hour and the 180th hour–200th hour, the L1-SW method cannot fit the original wind power signal smoothly with a larger λ. It makes the ramp detection results distinctly rough when compared to the optimized SDA shown in Fig. 3(c) (only one ramp by L1-SW and actually seven ramps by the optimized SDA).

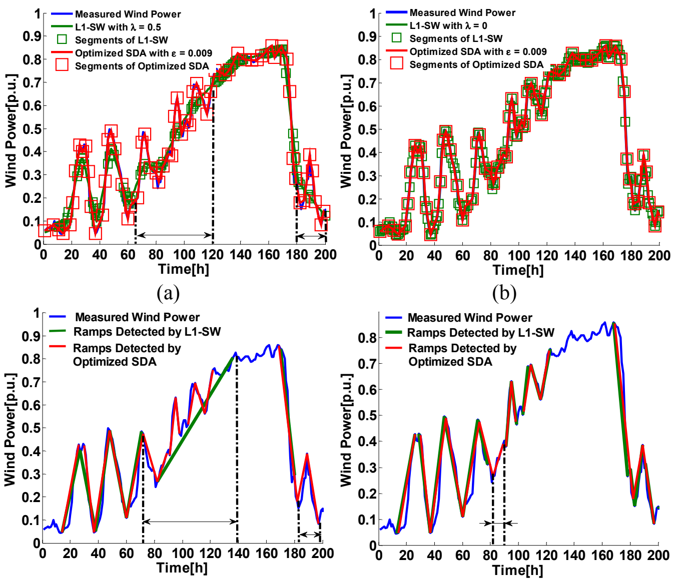

Fig. 3. Results of segments and significant ramps in the comparison of L1-SW to the optimized SDA. The subfigures (a) and (b) stand for approximated segments with λ={0.5, 0}, γ=5×10^{-6}, and ε=0.009, respectively. (a) λ=0.5; (d) λ=0. The subfigures (c) and (d) stand for extracted significant ramps with λ ={0.5, 0}, γ=5×10^{-6}, and ε=0.009, respectively. (c) λ=0.5; (d) λ=0.

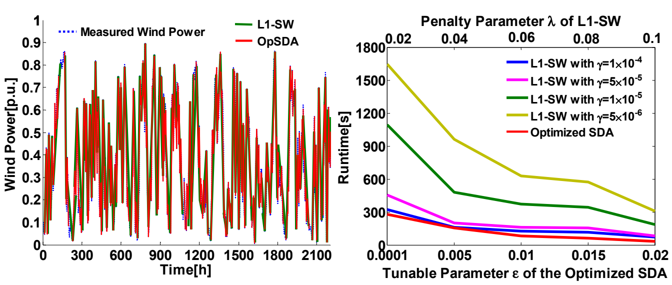

Fig. 4. (a) Sample results of ramp detection within one year of wind power data; (b) Runtime comparison of L1-SW with the parameter $\lambda \in [0.02, 0.1]$, γ= [1×10^{-4}, 5×10^{-5}, 1×10^{-5}, 5×10^{-6}] to the optimized SDA with the parameter $\varepsilon \in [0.0001, 0.02]$.

Fig. 4(a) shows all the ramps detected within the one-year period; Fig. 4(b) compares the runtime of the two methods (L1-SW with the up x-axis and the optimized SDA with the down x-axis). Although the detection results in L1-SW (Fig. 3 (b) and (d)) are accurate by visual inspection (only one ramp was not detected between the 80th hour and 90th hour) with a small enough γ, the runtime of L1-SW (Fig. 4(b)) is more than 25 minutes when λ is less than 0.02 (with γ=5×10^{-6}). However, the runtime of the optimized SDA with ε=0.009 is only 100 seconds. Overall, both the ramp detection performance and the runtime of L1-SW are sensitive to the penalty parameter λ and the threshold γ; whereas the runtime of the optimized SDA is less sensitive to the parameter ε.

C. Specific Ramps Comparison of the L1-SW, Original SDA, and Optimized SDA

To specifically illustrate the effectiveness of the optimized SDA, Fig. 5 shows more detailed ramp detection information within the first 150 hours. Three time intervals are enumerated: 12th hour–28th hour, 36th hour–49th hour, and 80th hour–140th hour, respectively, in Figs. 5(a), 5(b), 5(c), and 5(d). A set of parameters with two λ (0.5 and 0) and one ε (0.009) are used.

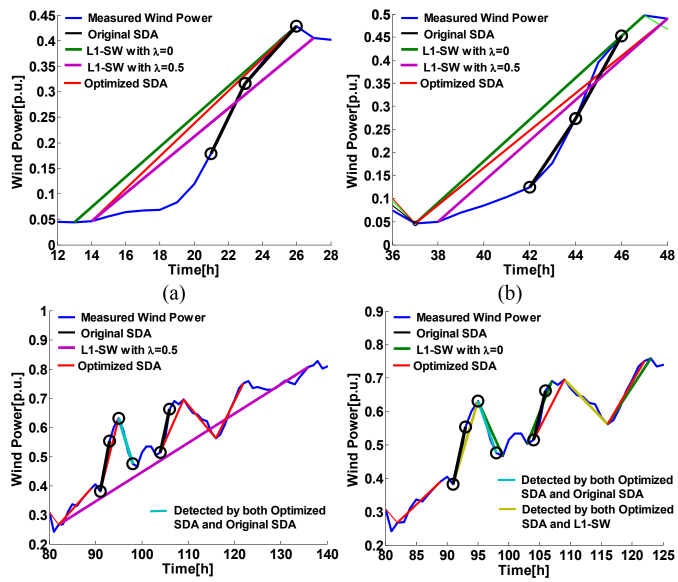

(c) (d)

Fig. 5. Specific ramps comparison with the L1-SW, original SDA, and optimized SDA. The subfigures (a) and (b) stand for two independent cases in the 12th hour–28th hour and 36th hour–49th hour, respectively. (a) λ=0.5, γ=5×10^{-6}, and ε=0.009; (b) λ=0, γ=5×10^{-6}, and ε=0.009. The subfigures (c) and (d) stand for a same case in the 80th hour–140th hour, with λ={0.5, 0}, γ=5×10^{-6}, and ε=0.009. (c) λ=0.5; (d) λ=0.

Figs. 5(a) and 5(b) indicate that the optimized SDA can combine the two ramps detected by the original SDA into one ramp. Meanwhile, the green and purple lines (by L1-SW) are almost similar, with the red line (by the optimized SDA) according to key ramp features such as start times, durations, rates, and magnitudes.

For better visualization, the L1-SW method with the two λ values (0.5 and 0) is plotted in Figs. 5(c) and 5(d), respectively. An additional label is used when a ramp is identified by two methods (e.g., the dark green line in Fig. 5(c) represents ramps detected by both the optimized SDA and the original SDA). In Fig. 5(c), six significant ramps are detected by the optimized SDA and three significant ramps are detected by the original SDA. However, only one significant ramp is detected by

L1-SW with a larger λ (0.5). In Fig. 5(d), five ramps are detected by L1-SW with a smaller λ (0).

Fig. 6 shows the numerical statistical analysis of the three key ramp features (duration, rate, and magnitude) based on the annual wind data. It is observed that the optimized SDA and L1-SW have similar probability density distributions (of ramp duration, rate, and magnitude) for both the up-ramps and down-ramps. However, the original SDA has a shorter ramp duration of three hours (with the highest frequency in Fig. 6(a)) without any segments of combination and optimization.

For offline analysis and detection of significant ramps, both the optimized SDA and the L1-SW (with a small γ value) can be utilized to provide good ramp detection performance for long-time dispatching problems; however, the optimized SDA is more preferable because of its short computation time. This is important for spatial analysis too, in which many SDAs might be working in parallel.

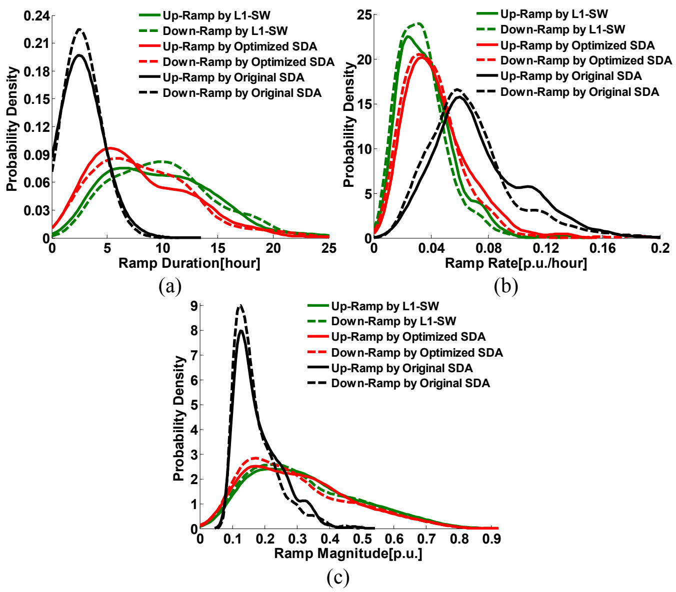

Fig. 6. Probability density distributions of the ramp features for up-ramps and down-ramps detected by the L1-SW, original SDA, and optimized SDA. The subfigures (a), (b), and (c) stand for ramp duration distributions, ramp rate distributions, and ramp magnitude distributions, respectively.

IV. Application of the Optimized SDA for Tuning the ε Parameter

The original SDA, which requires only one tunable parameter ε, has the advantage of computational and structural simplicity; this is a favorable attribute considering its robustness, even with noisy data [7]. Sometimes the original SDA without any optimization is preferable because of its inexpensive computation. Currently, this tunable parameter ε has been set only by heuristics based on expertise. It would be uniquely helpful to develop a framework for adaptively selecting the best ε value. In this paper, the proposed optimized SDA is used as a baseline to determine the optimal value of the tunable parameter ε_{opt}. The solving procedure is to make the ramp information detected by the original SDA with ε_{opt} in accordance with that detected by the optimized SDA.

Generally, with a smaller ε value, the fitting errors between the SDA approximated power and the actual power will be smaller. However, an ε value that is too small may divide a single significant ramp into multiple small ramps that do not satisfy the WPRE ramp definitions.

TABLE I
Contingency Table for the Original and Optimized SDA

	Optimized YES	Optimized NO	Total
Original YES	TP (*hits*)	FP (*false alarm*)	TP+FP
Original NO	FN (*misses*)	TN	FN+TN
Total	TP+FN	FP+TN	N=TP+FP+FN+TN

To determine the optimal parameter, ε_{opt}, based on the optimized SDA, a suite of WPRE detection metrics were used to evaluate the performance of ramp extraction with different ε values. The adopted metrics include probability of detection (POD), critical success index (CSI), frequency bias score (FBIAS), and success ratio (SR) [10], [16]. In this paper, the metrics are calculated based on a contingency table that provides a measure of skill for the original SDA approaching the optimized SDA. Table I is a contingency table that summarizes the results of different ε values. True positive (TP) represents the number of ramps detected by the original SDA (Original YES) that are accurately detected by the optimized SDA (Optimized YES); false positive (FP) is the number of ramps detected by the original SDA (Original YES) that are not detected by the optimized SDA (Optimized NO); false negative (FN) represents the number of ramps detected by the optimized SDA (Optimized YES) that are not extracted by the original SDA (Original NO); true negative (TN) is the number of non-occurring events for both the original and optimized SDA; and N is the total number of events.

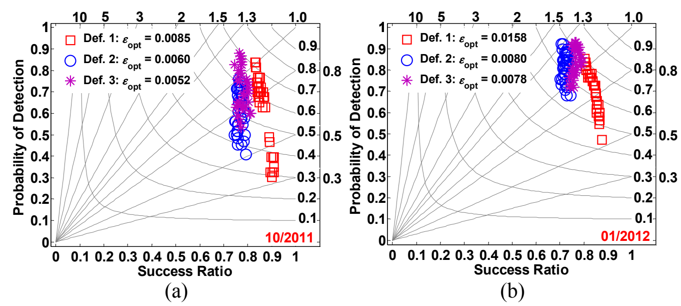

Fig. 7. Ramp detection performance with the optimal parameters. The subfigures (a) and (b) show optimal parameters defined by three ramp definitions in Oct. 2011 and Jan. 2012, respectively.

After calculating all of the metrics (POD, CSI, FBIAS, and FAR), the optimal ε value is determined by the largest POD and SR, which can be visualized on a performance diagram, as shown in Fig. 7. A performance diagram is used to understand the evolution of the original SDA with different ε values. To find the optimal parameter, ε_{opt}, the points in Fig. 7 move forward to the top right corner of the performance diagrams. Fig. 7 shows the optimal parameters of two months using 15-minute resolution data by three ramp definitions [10]:

(i) Significant Ramp Definition 1—the change in wind power output is greater than 5% of the installed wind capacity.

(ii) Significant Ramp Definition 2—the change in wind power output is greater than 5% of the installed wind capacity within a time span of 2.5 hours or less.

(iii) Significant Ramp Definition 3—a significant up-ramp is defined as the change in wind power output greater than 5% of wind capacity within a time span of 2.5 hours or less; a significant down-ramp is defined as the change in wind power output greater than 3% of wind capacity within a time span of 2.5 hours or less.

The results in Fig. 7 show that the original SDA can closely reach the top right corner of the performance diagrams with the optimal parameter, ε_{opt}, to provide a reasonable ramp extraction performance. The final adaptive ε_{opt} values of the study period spanning from October 2011 to September 2012 are plotted in Fig. 8, which can be used by power system operators.

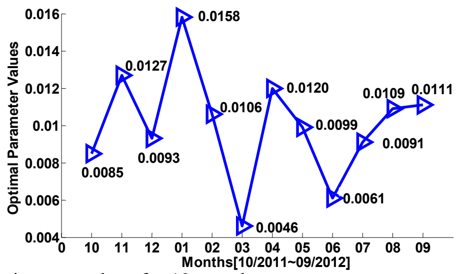

Fig. 8. Adaptive ε_{opt} values for 12 months.

TABLE II
SENSITIVITY INTERVAL OF FOUR DIFFERENT MONTHS

Month	Sensitivity Interval
10/2011	[0.005, 0.011]
01/2012	[0.006, 0.018]
04/2012	[0.010, 0.018]
07/2012	[0.005, 0.016]

The start point of the ε value is first predefined between 0.0001 and 0.02. Through computational experiments, a smaller starting interval is found to ensure the final performance of the original SDA, which is called the "sensitivity interval." In this study, the sensitivity interval is determined based on the POD and SR values, POD>0.75 and SR>0.75. TABLE II lists the sensitively intervals of four study months. When the tunable parameter is chosen from this sensitivity interval, the performance of the original SDA with ε_{opt} is less sensitive to the start value of ε.

V. CONCLUSION

An optimized SDA was developed in this paper for wind power detection. The developed optimized SDA was compared to the original SDA and the L1-SW methods in a case study of wind power at ERCOT. The results showed that the optimized SDA successfully identified wind power ramps and performed significantly better than the original SDA. The optimized SDA provided equal to better performance than the L1-SW method and with much less computational time. The developed optimized SDA was also used as a baseline to determine the optimal value of the tunable parameter in the original SDA, which could be performed offline. Then the selected optimal value ε_{opt} could be used for ramp detection.

In future work, more verification tests will be made to justify the robustness and stationarity of these historically learned parameters on wind power data. This proposed method and corresponding results can also be involved in unit commitment (UC) problems, ramp capability products, and even solar power. In addition, future work will merge "bumps" (non-WPREs with very short time durations, tiny ramp magnitudes, and opposite ramping directions) into the adjacent segments in the process of dynamic programming for better ramp detection.

ACKNOWLEDGEMENTS

This work was supported by the U.S. Department of Energy under Contract No. DE-AC36-08-GO28308 with the National Renewable Energy Laboratory. This work was also supported by the National Basic Research Program of China (2012CB215101).

REFERENCES

[1] P. Sorensen, N. A. Cutululis, A. Vigueras-Rodriguez, L. E. Jensen, J. Hjerrild, M. H. Donovan, and H. Madsen, "Power fluctuations from large wind farms," *IEEE Trans. Power Syst.*, vol. 22, no. 3, pp. 958-965, Aug. 2007.

[2] D. Lew, G. Brinkman, E. Ibanez, B.-M. Hodge, and J. King, "The western wind and solar integration study phase 2," presented at the 11th Annual International Workshop on Large-Scale Integration of Wind Power Into Power Systems as Well as on Transmission Networks for Offshore Wind Power Plants, Lisbon, Portugal, Sep. 2012.

[3] N. Navid and G. Rosenwald, "Market solutions for managing ramp flexibility with high penetration of renewable resource," *IEEE Trans. Sustain. Energy*, vol. 3, no. 4, pp. 784-790, Oct. 2012.

[4] AWS Truewind, "AWS Truewind's final report for the Alberta forecasting pilot project," Albany, NY, Tech. Rep.. [Online]. Available: http://www.aeso.ca/downloads/Alberta_PP_Final_Report_AWST_Jun25.pdf.

[5] M. Cui, D. Ke, Y. Sun, D. Gan, J. Zhang, and B.-M. Hodge, "Wind power ramp event forecasting using a stochastic scenario generation method," *IEEE Trans. Sustain. Energy*, DOI: 10.1109/TSTE.2014.2386870, 2015.

[6] R. Sevlian and R. Rajagopal, "Detection and statistics of wind power ramps," *IEEE Trans. Power Syst.*, vol. 28, no. 4, pp. 3610-3620, Nov. 2013.

[7] Y. V. Makarov, C. Loutan, J. Ma, and P. Mello, "Operational impacts of wind generation on California Power Systems," *IEEE Trans. Power Syst.*, vol. 24, no. 2, pp. 1039-1050, May 2009.

[8] E. H. Bristol, "Swinging door trending: adaptive trend recording?" in *1990 Proc. ISA National Conference*, pp. 749-756.

[9] A. Florita, B. M. Hodge, and K. Orwig, "Identifying wind and solar ramping events," in *Proc. 2013 IEEE 5th Green Technologies Conf.*, Denver, CO, USA, pp. 4-5.

[10] J. Zhang, A. Florita, B.-M. Hodge, and J. Freedman, "Ramp forecasting performance from improved short-term wind power forecasting," presented at the ASME International Design Engineering Technical Conf. & Computers and Information in Engineering Conf. (IDETC/CIE 2014), Buffalo, NY, USA, Aug. 17-20, 2014.

[11] D. C. Barr, "The use of a data historian to extend plant life," in *1994 Proc. Int. Conf. Life Management of Power Plants*, U.K., Dec. 12-14, Heriot-Watt Univ.

[12] C. W. Potter, E. Grimit, and B. Nijssen, "Potential benefits of a dedicated probabilistic rapid ramp event forecast tool," in *2009 Proc. IEEE Power Syst. Conf. and Expo.*, Seattle, WA, USA, pp. 1-5.

[13] C. Kamath, "Understanding wind ramp events through analysis of historical data," in *2010 Proc. Transmission and Distribution Conf. Expo.*, New Orleans, LA, USA, pp. 1-6.

[14] J. Wilczak, M. Marquis, C. Finley, and J. Freedman, "The wind forecast improvement project (WFIP): A public/private partnership for improving short term wind energy forecasts and quantifying the benefits of utility operations," U.S. Department of Energy (DOE), Washington, D.C., Tech. Rep. DE-EE0003080, Apr. 2014.

[15] R. Sevlian and R. Rajagopal, "Wind power ramps: Detection and statistics," in *2012 Proc. IEEE PES GM*, San Diego, CA, USA, pp. 1-8.

[16] P. J. Roebber, "Visualizing multiple measures of forecast quality," *Wea. and Forecasting*, vol. 24, no. 2, pp. 601-608, Apr. 2009.